Schultz, R. M., Varma-Nelson, P., Ortiz, R., Kozlowski, K. A., Orawski, A. T., Pagast, P., & Frankfater, A. (1989) *J. Biol. Chem. 264*, 1497–1507.
Serjeant, E. P., & Dempsey, B. (1979) *Ionisation Constants of Organic Acids in Aqueous Solution*, Pergamon Press, New York.
Shaw, E. (1980) in *Enzyme Inhibitors as Drugs* (Sandler, M., Ed.) pp 25–42, University Park Press, Baltimore, MD.
Shaw, E. (1988) *J. Biol. Chem. 263*, 2768–2772.
Shaw, E. (1990) *Adv. Enzymol. Relat. Areas Mol. Biol. 63*, 271–347.
Shaw, E., & Ruscica, J. (1968) *J. Biol. Chem. 243*, 6312–6313.
Shaw, E., Angliker, H., Rauber, P., Walker, B., & Wikstrom, P. (1986) *Biomed. Biochim. Acta 45*, 1397–1403.
Silverman, R. B. (1988) *Mechanism-based Enzyme Inactivation: Chemistry and Enzymology*, Chapter 1, CRC Press, Inc., Boca Raton, FL.
Sloane, B. F., Lah, T. T., Day, N. A., Rozhin, J., Bando, Y., & Honn, K. V. (1986) in *Cysteine Proteinases and Their Inhibitors* (Turk, V., Ed.) pp 729–749, Walter de Gruyter and Co., New York.
Smith, R. A., Copp, L. J., Coles, P. J., Pauls, H. W., Robinson, V. J., Spencer, R. W., Heard, S. B., & Krantz, A. (1988a) *J. Am. Chem. Soc. 110*, 4429–4431.
Smith, R. A., Copp, L. J., Donnelly, S. L., Spencer, R. W., & Krantz, A. (1988b) *Biochemistry 27*, 6568–6573.
Smith, R. A., Coles, P. J., Spencer, R. W., Copp, L. J., Jones, C. S., & Krantz, A. (1988c) *Biochem. Biophys. Res. Commun. 155*, 1201–1206.
Stein, R. L. (1985) *J. Am. Chem. Soc. 107*, 5767–5775.
Streitwieser, A., Jr. (1962) *Solvolytic Displacement Reactions*, p 82, McGraw-Hill, New York.
Strong, L. E., Van Waes, C., & Doolittle, K. H. (1982) *J. Solution Chem. 11*, 237–258.
Strong, L. E., Brummel, C. L. & Lindower, P. (1987) *J. Solution Chem. 16*, 105–124.
Sunko, D. E., Jursič, B., & Ladika, M. (1987) *J. Org. Chem. 52*, 2299–2301.
Whitaker, J. R., & Perez-Villaseñor, J. (1968) *Arch. Biochem. Biophys. 124*, 70–78.
Wofsy, L., Metzger, H., & Singer, S. J. (1962) *Biochemistry 1*, 1031–1039.
Zumbrunn, A., Stone, S., & Shaw, E. (1988a) *Biochem. J. 250*, 621–623.
Zumbrunn, A., Stone, S., & Shaw, E. (1988b) *Biochem. J. 256*, 989–994.

^{2}H Nuclear Magnetic Resonance of the Gramicidin A Backbone in a Phospholipid Bilayer†

R. S Prosser and J. H. Davis*
Guelph-Waterloo Program for Graduate Work in Physics, Department of Physics, University of Guelph Campus, Guelph, Ontario, Canada N1G 2W1
F. W. Dahlquist and M. A. Lindorfer
Institute of Molecular Biology, University of Oregon, Eugene, Oregon 97403
Received December 5, 1990; Revised Manuscript Received January 23, 1991

ABSTRACT: Solid-state ^{2}H NMR spectroscopy has been employed to study the channel conformation of gramicidin A (GA) in unoriented 1,2-dimyristoyl-*sn*-glycerol-3-phosphocholine (DMPC) multilayers. Quadrupolar echo spectra were obtained at 44 °C and 53 °C, from gramicidin A labels in which the proton attached to the α carbon of residue 3, 4, 5, 10, 12, or 14 was replaced with deuterium. Because of the nearly axially symmetric electric field gradient tensor, the quadrupolar splittings obtained from an unoriented multilamellar dispersion of DMPC and singly labeled GA directly yield unambiguous orientational constraints on the C–^{2}H bonds. The average of the ratios of the quadrupolar splittings of the left-handed amino acids to those of the right-handed amino acids, $\langle \Delta\nu_{QL}/\Delta\nu_{QD} \rangle$, is expected to be 0.97 ± 0.04 for a relaxed right-handed $\beta_{LD}^{6,3}$ helix, while a ratio of 0.904 ± 0.003 is expected for a left-handed $\beta_{LD}^{6,3}$ helix. Since we have experimentally determined this ratio to be 1.01 ± 0.04, we conclude that the helix sense of the channel conformation of GA is right-handed. Assuming that the dominant motions are fast axial diffusion of the gramicidin molecule and reorientation of the diffusion axis with respect to the local bilayer normal, then the theoretical splittings may all be scaled down by a constant motional narrowing factor. In this case, a relaxed right-handed $\beta_{LD}^{6,3}$ helix, whose axis of motional averaging is roughly along the presumed helix axis, gave the best fit to experimental results. The reasonably uniform correspondence between the splittings predicted by the relaxed right-handed $\beta_{LD}^{6,3}$ helix and the observed splittings, for labels from both the inner and outer turn of GA, did not reflect a peptide backbone flexibility gradient, since an outer turn (i.e., the turn of the helix closest to the interface with the water) with greater flexibility would show additional motional narrowing for labels located there.

(Val$_1$)gramicidin A (GA)[1] is a pentadecapeptide consisting of 15 alternating L- and D-amino acids (Sarges & Witkop, 1965) and has the following chemical formula:

HCO-L-Val$_1$-Gly$_2$-L-Ala$_3$-D-Leu$_4$-L-Ala$_5$-D-Val$_6$-L-Val$_7$-D-Val$_8$-L-Trp$_9$-D-Leu$_{10}$-L-Trp$_{11}$-D-Leu$_{11}$-L-Trp$_{13}$-D-Leu$_{14}$-L-Trp$_{15}$-NHCH$_2$CH$_2$OH

Pure GA can be isolated in gram quantities from commercially

† This work has been supported by grants from the Natural Sciences and Engineering Research Council. R.S.P. would also like to acknowledge NSERC for graduate studies scholarships.

0006-2960/91/0430-4687$02.50/0

available gramicidin (Stankovic et al., 1990), or it (or indeed a host of labeled GA's or GA analogues) may be obtained, with high yields, by solid-phase peptide synthesis (Fields et al., 1989). Consequently, this peptide has served as a useful model in the study of integral membrane proteins, particularly in studies of structural/functional relationships, lipid–protein interactions (Chapman et al., 1977; Tanaka & Freed, 1985; Morrow & Davis, 1988; Tournois et al., 1988; Wang et al., 1988; Cornell & Separovic, 1988; Van Mau et al., 1988; Killian et al., 1989; Strässle et al., 1989; Cornell et al., 1989; Watnick et al., 1990), and ion-selective transmembrane channels (Roux & Karplus, 1988, and references 21–41 therein; Hinton et al., 1988, 1989; Heinemann & Sigworth, 1989; Åqvist & Warshel, 1989; Koeppe et al., 1990). However, a meaningful understanding of these features of an integral membrane protein system is dependent upon a dynamic three-dimensional picture of the protein in its membrane host. In this regard, X-ray crystallography is limited by the technology of crystallizing membrane proteins and, in the case of gramicidin, by the intermediate size range of the unit cell, which hampers conventional phasing methods, although both limitations are being gradually overcome (Gennis, 1989; Deisenhofer et al., 1985; Wallace & Ravikumar, 1988). High-resolution NMR has had limited success with certain peptides incorporated in organic solvents or detergent micelles [e.g., Arseniev et al. (1985)] although it remains to be seen whether the physical properties of the host solvent molecules adequately mimic the essential physical properties of biomembranes.

Unlike most diffraction techniques that require single crystals, solid-state NMR is particularly suited to the study of uniaxially oriented systems (Opella & Stewart, 1989), a situation that is relatively easy to achieve even in truly bilayer mimetic systems [e.g., Moll and Cross (1990)]. Furthermore, even large ordered systems or biological macromolecules that are immobile on NMR time scales (motions whose correlation times are longer than 10^{-6} s) may in principle be studied by this technique. Finally, via spectral lineshape analysis and relaxation experiments, solid-state NMR permits local and global motions to be observed on a time scale ranging from 10^{-10} s to 1 s. However, it is expected that it will be necessary to study more than one type of nucleus to construct a model-independent picture of a membrane protein [e.g., Opella and Stewart (1989)].

The currently accepted channel conformation of gramicidin A is that of a head-to-head dimerized pair of $\beta^{6.3}_{LD}$ helices (Venkatachalam & Urry, 1983, 1984). Ion-induced chemical shifts and energetic considerations have led Urry and coworkers (Urry et al., 1982; Venkatachalam & Urry, 1983) to conclude that the helix sense of GA must be left-handed. A two-dimensional ^{1}H NMR study of the Na^+ complex of GA in detergent micelles has revealed the structure to approximate a right-handed $\beta^{6.3}_{LD}$ helix, with a slightly irregular detailed structure (Arseniev et al., 1985). From ^{13}C chemical shift anisotropies of various carbonyl labeled GA's in oriented phospholipid bilayers, Cornell and co-workers concluded that the predicted orientations of the labeled carbonyl groups with respect to the presumed helix axis are consistent with a $\beta^{6.3}_{LD}$ helix (Cornell et al., 1988; Smith et al., 1989). These same authors also reported that, although the peptide behaves largely as a rigid barrel, segments of the peptide close to the membrane surface possess greater motional freedom. After incorporation of ^{15}N-labeled residues at the Val_1, Gly_2, Ala_3, Leu_4, Ala_5, Val_6, or Val_7 position of GA, ^{15}N NMR spectroscopy was employed by Nicholson and Cross (1989) on oriented DMPC multilamellar dispersions of these GA dimers to verify the β-sheet hydrogen-bonding pattern originally proposed by Urry et al. (1971). Additionally, from the evaluation of measured ^{15}N chemical shift resonances, they were able to conclude that the helix sense of the "cation-free" channel conformation of GA was right-handed.

^{2}H NMR has been employed on exchange-labeled GA in both DPPC multilayers (Datema et al., 1986) and in an oriented lyotropic nematic phase (Davis, 1988). Because of ambiguities in resolving, let alone assigning, all of the doublets, the results of Davis were tentatively postulated to be consistent with a rigid slightly distorted $\beta^{6.3}_{LD}$ helix undergoing axially symmetric reorientation about the director of the liquid-crystalline phase with a correlation time of about 10^{-7} s. Hing et al. (1990a,b) avoided the assignment dilemma by studying synthetic GA labels in which either the proton attached to the formyl group carbon or to the α carbon of Ala_3 was replaced by deuterium. Proton-decoupled quadrupolar echo spectra were acquired on oriented multilayer DMPC dispersions of these labeled GA molecules in both the gel and liquid-crystalline phases. Assuming that the only significant motion was fast rotational diffusion of the dimer about the axis of the helix, the observed quadrupolar splitting of the Ala_3-labeled peptide was consistent with a $\beta^{6.3}_{LD}$ helix. However, the splitting corresponding to the formyl-labeled peptide was inconsistent with a left-handed $\beta^{6.3}_{LD}$ helix undergoing only fast axial rotation (Hing et al., 1990b). Without additional labels or relaxation data, the extent of motional narrowing could not be assessed, and hence it was impossible for the authors to discriminate between the left- and right-handed versions of the $\beta^{6.3}_{LD}$ helix. Macdonald and Seelig (1988) have also employed ^{2}H NMR on GA in a DMPC/GA/water multilayer system. In this case, the aromatic ring systems of all four tryptophan side chains were deuterated. From their measurements of the quadrupole echo relaxation time, a rotational correlation time of 2×10^{-7} s was estimated for the dimer.

In this study of GA in a phospholipid multilayer, we have chosen to apply solid-state ^{2}H NMR to the problem of the backbone structure and dynamics of the channel conformation of GA in DMPC/water multilamellar dispersions. Six GA molecules were synthesized in which the proton attached to the α carbon of each of the two alanine and four leucine residues was replaced with deuterium. In addition, a doubly labeled sample was prepared in which α carbon protons in both of the alanines were replaced with deuterium. The splittings obtained from this sample are compared to those of the singly labeled gramicidins. The spectral lineshape obtained from a quadrupolar echo experiment provides a qualitative measure of the time scale of the dominant motions, while the splitting gives the orientation of the C_α–^{2}H bond with respect to the axis of motional averaging, without the need for preparing oriented multilayers. The next section describes the sample preparation and the experimental methods used in obtaining these ^{2}H NMR spectra and the ^{1}H NMR and circular dichroism experiments that were performed in order to assure that GA adopts the channel conformation. We then present our results and discuss the implications of our spectra in terms of structural and dynamical constraints for five structural

[1] Abbreviations: GA, gramicidin A; DMPC, 1,2-dimyristoyl-*sn*-glycero-3-phosphocholine; DMF, *N*,*N*-dimethylformamide; HPLC, high-performance liquid chromatography; HMP, *p*-hydroxymethylphenoxyacetic acid; TMS, tetramethylsilane; NMR, nuclear magnetic resonance; CD, circular dichroism; COSY, coherence spectroscopy; DMSO, dimethyl sulfoxide; *S*/*N*, signal-to-noise ratio; FID, free induction decay; MDS, molecular dynamics simulation; Fmoc, 9-fluorenylmethoxycarbonyl.

models of the channel conformation of GA: Urry's left- and right-handed $\beta^{6.3}_{LD}$ helices (unrelaxed), the left- and right-handed $\beta^{6.3}_{LD}$ helices run on a molecular dynamics simulation for 80 ps (relaxed) (Chiu et al., 1990), and Arseniev's right-handed helical dimer.

Materials and Methods

Sample Preparation. Gramicidin is notorious for adopting various metastable conformational states in hydrated phospholipid bilayers (Masotti et al., 1980; Wallace, 1983; Killian & Urry, 1988; LoGrasso et al., 1988; Sawyer et al., 1990) that may generally be converted to the stable conformation after extensive heating is applied to the phospholipid dispersion. A number of factors may determine the conformation that GA ultimately adopts in a phospholipid dispersion, among them, the type of phospholipid host, the solvent used to cosolubilize the phospholipid and GA, the incubation temperature, and the peptide/lipid ratio. Thus a rigorous sample preparation regimen was used, following that of LoGrasso et al. (1988), in order that the stable channel conformation of GA was obtained, as determined by circular dichroism (CD).

For circular dichroism measurements, we used synthetic gramicidin A (described below) and gramicidin D (Dubos) purchased from Sigma Chemical Co. (St. Louis, MO), while DMPC was purchased from Avanti Polar Lipids Inc. (Birmingham, AL); all were used without further purification. For both CD and ^{2}H NMR, the gramicidin/DMPC samples were first codissolved (in a 1:10 molar ratio) in 99.5+% NMR grade trifluoroethanol (Aldrich Chemical Co., WI) at a concentration of about 6 mL of trifluoroethanol per 0.15 g of dry sample and left at 38 °C for 40 min. The bulk of the solvent was then removed by rotary evaporation and the remainder was removed by drying under vacuum for at least 12 h. For the CD experiments, deionized water or 20 mM phosphate buffer was then added to the dry sample at a concentration of 2.5 mL of H_2O per milligram of gramicidin. The sample was next warmed to 40 °C and gently stirred for 2 h, sonicated at 8 W for 30 min at 40 °C, and then diluted by a factor of 10, before being centrifuged to remove large light-scattering aggregates. For the ^{2}H NMR experiments, 20 mM phosphate buffer was added to the dry sample at a 4/3 ratio (by mass) of water to dry sample. The NMR sample was next gently stirred, until it was uniformly white in color, and left overnight at −20 °C, in order to prepare large multilamellar dispersions. Before any ^{2}H NMR experiments were initiated, the dispersion was typically incubated at 53 °C for a few hours; the order of the ^{2}H NMR experiments was always from high temperature (53 °C) to some lower temperature (typically 44 °C). Typically 100 mg of GA was used for a single ^{2}H NMR sample.

Preparation of ^{2}H-Ala and ^{2}H-Leu. Amino acids were deuterium labeled by first racemizing *N*-acetyl-L-alanine (or *N*-acetyl-L-leucine) in d_1-acetic acid/acetic anhydride solution as described in Greenstein and Winitz (1961). Resolution of the two isomers was accomplished by hydrolyzing the L-isomer with porcine renal acylase (acylase I, grade 1, Sigma Chem. Co., St. Louis, MO) and crystallization of the L-amino acid from 80% ethanol (for alanine) or 50% ethanol (for leucine).

The *N*-acetyl-D-d_1-alanine (or *N*-acetyl-D-d_1-leucine) was separated from any residual free L-amino acids by elution in distilled deionized water (pH 6–7) through a Dowex 50 ion-exchange column (Aldrich, Milwaukee, WI). The *N*-acetyl-D-d_1-alanine (or *N*-acetyl-D-d_1-leucine) was refluxed over gentle heat in a 10-fold amount of 2 N HCl for 2 h. The pH was then adjusted to about 5 with pyridine. After the amino acid was redissolved by heating, an equal volume of hot absolute ethanol was added. After being cooled for several hours, the amino acid was removed by filtration, and the D-d_1-amino acid was then recrystallized from 80% ethanol (for alanine) or 50% ethanol (for leucine) (Greenstein & Winitz, 1961).

The extent of hydrolysis by the acylase was monitored by high-resolution ^{2}H NMR, the optical purity of the L- and D-amino acids and their *N*-acetyl derivatives was checked by polarimetry in a glacial acetic acid solution. In all cases, the molecular rotations measured were within 4% of the expected values (Greenstein & Winitz, 1961). The results of each step of the reaction were also monitored by high-resolution ^{1}H NMR at 300 MHz.

Solid-Phase Peptide Synthesis of Gramicidin A. Amino acids deuterated at the α carbon were protected by reaction with 9-fluorenylmethylchloroformate in a Na_2CO_3/dioxane solution as described in Stewart and Young (1984). Unlabeled Fmoc amino acids were purchased from Bachem Bioscience, Inc. Solvents [methylene chloride, *N*,*N*-dimethylformamide (DMF), methanol] for solid-phase synthesis and for HPLC were HPLC grade, purchased from Burdick and Jackson. *p*-Hydroxymethylphenoxyacetic acid resin and all other solid-phase synthesis reagents were purchased from Applied Biosystems. Deuterium-labeled gramicidin A was synthesized on an Applied Biosystems Model 430A synthesizer (Applied Biosystems) using hydroxybenzotriazole active esters and Fmoc acid-terminal protection, closely following the procedure described by Fields et al. (1989). Residues Ala_3, Leu_4, and Ala_5 were coupled twice, both times in DMF. Cleavage from the resin (0.5 gm) was in 50% ethanolamine in DMF (5 mL) overnight at 50 °C with stirring (Fields et al., 1989). The resin was filtered and rinsed twice with 5 mL of DMF. The filtrate volume was reduced by half with rotary evaporation. Gramicidin A was precipitated by addition of a 20-fold excess of water; the precipitate was filtered and dried overnight under vacuum. Analytical HPLC was performed on a Beckman Ultrasphere ODS column (46 × 150 mm) using 85% methanol/15% 0.1 M NaH_2PO_4 at pH 2.5 with a flow rate of 0.7 mL/min (Fields et al., 1989). All synthesis products gave a sharp single peak corresponding to gramicidin A with only minor impurity peaks with the exception of the first attempt at (d_1-Leu_{14})gramicidin A. For this reason, we repeated the synthesis for this label position. The second synthesis yielded a clean HPLC chromatogram, so the first preparation was discarded.

Amino acid analysis after acid hydrolysis (Bidlingmeyer et al., 1984) yielded results close to the nominal amino acid composition of gramicidin A, except for tryptophan, which was destroyed during hydrolysis. Two of the penultimate peptide-resin samples (immediately prior to addition of formylvaline) were sequenced on an Applied Biosystems Model 475 protein sequencer. The results were consistent with the correct sequence.

^{1}H NMR Experiments. About 2 mg of each of the synthetic gramicidin-A preparations were dissolved in about 0.25 mL of d_6-dimethyl sulfoxide. One-dimensional ^{1}H spectra at 500.1 MHz were identical with that of commercial gramicidin D in d_6-DMSO. Either two-dimensional ^{1}H COSY or double-quantum filtered COSY spectra (Ernst et al., 1987) were also acquired at 500.1 MHz for each of the synthetic peptides. These spectra indicated that, at least in DMSO, the synthetic peptides adopted the same conformation as gramicidin D, and from the diminution of the appropriate cross-peaks in the fingerprint region (the area from about 7 to 9 ppm downfield from TMS, the amide region, in the first dimension, and from

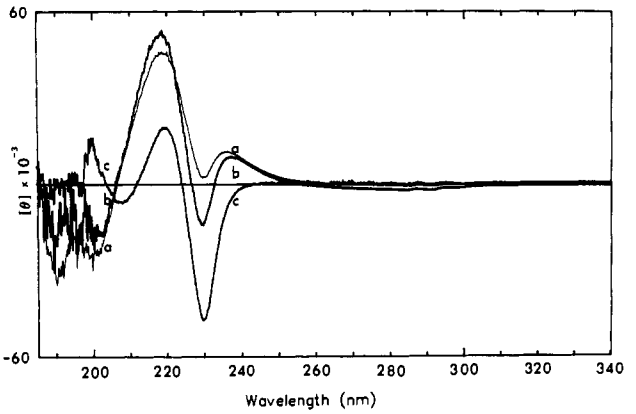

FIGURE 1: CD spectra at 46 °C of sonicated dispersions of gramicidin and DMPC in a 1:10 peptide-to-lipid molar ratio, with 20 mM pH 7.0 phosphate buffer as a solvent. Samples were prepared by using TFE (a and b) or methanol (c) to codissolve the peptide and lipid. Either gramicidin D (a and c) or gramicidin A (b) was used as the peptide.

about 2 to 5 ppm, the $C_\alpha H$ region, in the second dimension) that the peptides were labeled as expected.

CD Experiments. CD spectra were recorded at 46 °C, with a J-600 spectropolarimeter (Japan Spectroscopic Co., Tokyo). Figure 1, traces a and c, contains CD spectra obtained under exactly the same conditions except that trifluoroethanol and redistilled methanol were used, respectively, as the cosolubilizing solvent. Trace a reproduces the generally accepted profile for the channel state of the gramicidin D mixture (LoGrasso et al., 1988). The CD trace labeled b in Figure 1 was obtained under exactly the same conditions as that in trace a except that the peptide used was our synthetic GA; the slight differences between traces a and b are not surprising considering that gramicidin D contains approximately 85% GA and 15% gramicidins B and C, which differ in the substitution of Trp_{11} with phenylalanine or tyrosine. The CD spectrum shown in Figure 1b faithfully reproduces the generally accepted profile for the channel state of GA [see Wallace (1983) and Killian and Urry (1988)]. With this result and with our ^1H NMR data, we can therefore be confident that the synthetic GA samples are identical with GA, except for the deuterium labels, and that our sample preparation methods result in the channel state of GA.

^2H NMR Experiments. The ^2H NMR spectra were all acquired on a home-built spectrometer operating at 55.26 MHz, corresponding to a magnetic field of 8.5 T. In all cases, the quadrupolar echo technique was employed (Davis et al., 1976). The 90° pulses used in the quadrupolar echo sequences were always between 2.5 and 3.0 μs, while the repetition time used was 0.4 s and the interpulse spacing was 35.0 μs, unless otherwise stated. Typically 400 000 scans were needed to obtain a spectrum with a signal-to-noise ratio (S/N) sufficient to observe the shoulders in the powder pattern (taking about 2 days).

Complex free induction decay signals (FID's), obtained from the quadrupolar echo experiments, were analyzed with software adapted from that of Dennis Hare (Hare Research, Woodinville, WA). An automatic phase-correct algorithm adjusts the complex FID such that the absorption signal lies completely in the real part of the FID while the dispersion signal lies in the imaginary part. By use of the last few points of the FID, the baseline offset was automatically adjusted to zero, after which a Traficante resolution-enhancement apodization function was employed (Traficante, 1987).

To obtain an undistorted spectrum, it is important to acquire the quadrupolar echo signal in such a way that one of the sampled points lies precisely at the top of the symmetric echo and to use that point as the first time domain point when performing the Fourier transformation. Davis (1983) described a method of shifting (or symmetrizing) the echo after acquisition, making it unnecessary to empirically adjust the echo delay or digitizer trigger delay. The procedure used is actually a length-five finite impulse response digital filter (Oppenheimer & Schafer, 1975), which results in a smoothing of the data (Neilson, 1964). If, in addition, one oversamples the echo by a factor of M, then it will be possible to separate the sequence of N points (1,2,3,...,N) into M subsequences each of N/M points

$$(1, 1 + M, 1 + 2M, ..., 1 + [N/M]M - M)$$

$$(2, 2 + M, 2 + 2M, ..., 2 + [N/M]M - M)$$

...

$$(M, M + M, M + 2M, ..., M + [N/M]M - M)$$

Each of the subsequences can be separately shifted and Fourier transformed to yield the NMR spectrum. If the bandwidth of the receiver system (including the preamplifer and the probe) is greater than or equal to the Nyquist frequency for the oversampling rate, then separating, shifting, and adding the subsequences generated as described above can result in an improved signal-to-noise ratio. This digital filtering (or contraction) procedure can be used in lieu of an analogue filter. All of the spectra to be presented in this study were obtained by employing the contraction procedure with $M = 3$ and with our analogue filters at 350 kHz.

Results and Discussion

In this section, we investigate the extent to which the ^2H NMR spectra of the backbone-labeled GA's are consistent with five different models of the channel conformation of GA: Urry's left- and right-handed $\beta^{6.3}_{LD}$ helices, the left- and right-handed $\beta^{6.3}_{LD}$ helices relaxed by MDS, and the right-handed Arseniev model. Figure 2 depicts the ZX and ZY perspectives of the backbone of Urry's theoretical left-handed $\beta^{6.3}_{LD}$ helix, while Figure 3 represents the corresponding right-handed counterparts, relaxed by a molecular dynamics simulation (MDS) for 80 ps (Chiu et al., 1990). The molecular dynamics simulations incorporated water molecules inside the GA channel and the channel ends (representing bulk water), while the lipid molecules were accounted for by artificial restraints imposed on the motions of the polypeptide. The atomic coordinates for these models were obtained from the lab of E. Jakobsson (Urbana, IL) and were adapted for our purposes by first removing all side-chain atoms and then solving for the coordinates of the protons attached to the α carbons of the Val, Ala, Leu, and Trp residues. This was done by using the angles formed between the $H–C_\alpha$ bond and the adjacent directly bonded nitrogen, carbonyl carbon, and side-chain atom, obtained from X-ray files of the various amino acids on a software package called MACROMODEL (Columbia University, NY). Each model was then rotated about the Z axis (helix long axis) until the first α carbon of the monomer appearing at the bottom left of the figure lay in the ZX plane. The asterisks in Figures 2 and 3 represent positions of protons attached to α carbons of the valine, alanine, leucine, and tryptophan residues. Although we are reporting only on the results of experiments performed on ($^2H–C_\alpha$)Ala_3, -Ala_5, -Leu_4, -Leu_{10}, -Leu_{12}, and -Leu_{14} GA labels, we are currently in the process of synthesizing ($^2H–C_\alpha$)Val_1, -Val_6, -Val_7, -Val_8, -Trp_9, -Trp_{11}, -Trp_{13}, and -Trp_{15} GA labels. Note from Figures 2 and 3 that the left-handed helices can be readily distinguished from their right-handed counterparts by the roughly opposite

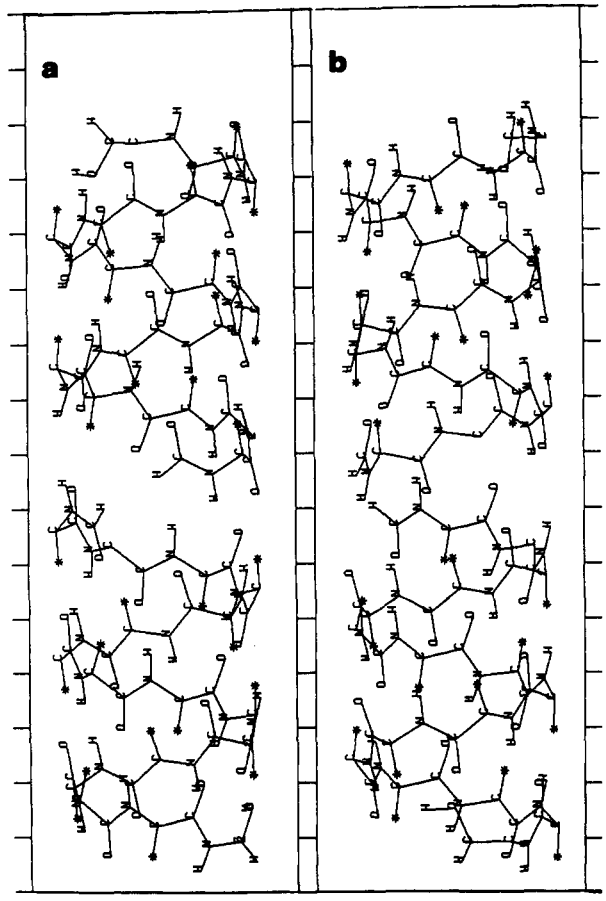

FIGURE 2: ZX (a) and ZY (b) perspectives of the left-handed $\beta^{6,3}_{LD}$ helix model for GA. The Z axis represents the helical axis (or the best approximation to the helical axis for all those models that represent irregular helices). Asterisks represent positions of protons attached to the α carbons of the valine, alanine, leucine, and tryptophan residues. Grids are marked off at 2-Å intervals. In order to compare the models, all have been rotated about the Z axis in order that the first α carbon of the monomer to the reader's bottom left lies in the ZX plane (Y = 0) such that it appears at the lefthand edge of each of the ZX perspectives of the figures.

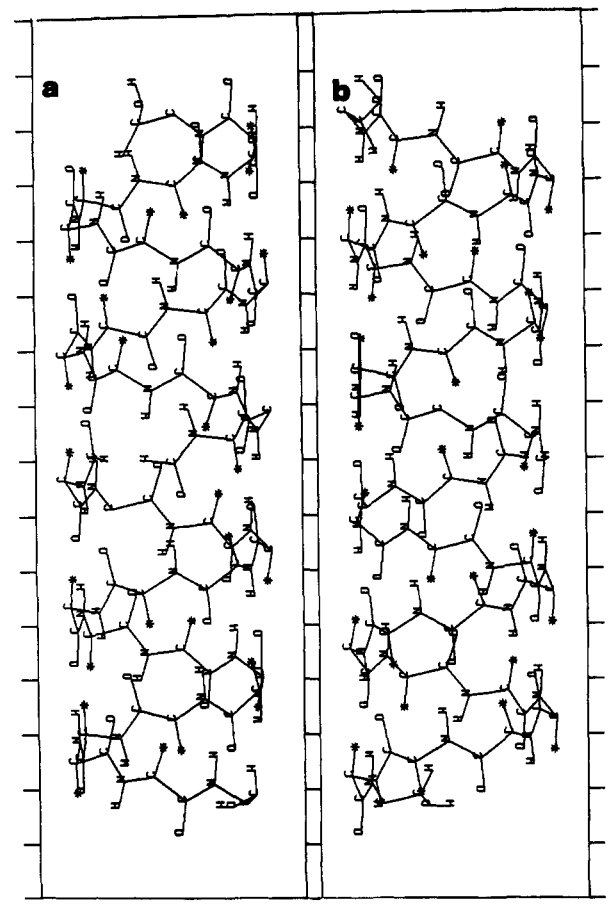

FIGURE 3: ZX and ZY perspectives of the right-handed $\beta^{6,3}_{LD}$ helix (a and b, respectively) run on a molecular dynamics simulation for 80 ps (Chiu et al., 1990).

direction of the C_α-^{2}H, C=O, and N-H bonds, leaving the labels with significantly different local environments.

The magnitude of the ^{2}H quadrupolar splitting measured from a powder pattern is given by the equation (Davis, 1983)

$$\langle \Delta\nu_Q \rangle = \frac{3}{8}\frac{e^2qQ}{h}\langle [(3\cos^2\theta) - 1] + \eta\cos 2\alpha \sin^2\theta \rangle \quad (1)$$

where e^2qQ/h = 168 kHz is the quadrupolar coupling constant and the asymmetry parameter η is defined by the relation $\eta \equiv |(V_{xx} - V_{yy})/V_{zz}|$, where $|V_{zz}| \geq |V_{xx}| \geq |V_{yy}|$ so that $0 \leq \eta \leq 1$. Here, the V_{ii} are the principal components of the electric field gradient (EFG) tensor at the ^{2}H nucleus. The angles α and θ define the orientation of the EFG principal axis system with respect to the symmetry axis of the bilayer. In the presence of rapid axially symmetric reorientation about the symmetry axis, α in eq 1 takes on all values so that the term proportional to η averages to zero. The ^{2}H NMR spectra of the GA labels in this study are all consistent with rapid axially symmetric reorientation. In this case, we can write

$$\langle \Delta\nu_Q \rangle = \frac{3}{8}\frac{e^2qQ}{h}\langle (3\cos^2\theta) - 1 \rangle \quad (2)$$

For a rigid molecule simply undergoing rapid axially symmetric reorientation about a single axis, the quadrupolar splittings would be independent of temperature, so long as the motion was rapid on the ^{2}H NMR time scale. However, the spectra shown in Figure 4 for (^{2}H-C_α)Leu$_{12}$ GA at 53.0 °C (a), 44.0 °C (b), and 20.6 °C (c) suggest that, although the motion is rapid on the ^{2}H NMR time scale, there is a slight temperature dependence of the splittings. From 53 °C to 20.6 °C, the splitting is observed to change from 98.7 kHz to 100.2 kHz, a difference of 1.5%. For this reason, we propose that, in addition to rapid axially symmetric reorientation of this rigid molecule about the symmetric axis, the symmetry axis itself fluctuates with respect to the direction of the external magnetic field (Davis, 1988). This additional motion might arise from libration of the rigid molecule in a liquid-crystalline host. In this case, the splittings will be a function of temperature. However, the ratio of any two splittings, under this two-motion model, will be independent of temperature (Davis, 1988), and in particular the ratio of the quadrupolar splitting for a left-handed amino acid label to that of a right-handed amino acid label, $\langle \Delta\nu_{QL}/\Delta\nu_{QD} \rangle$, will be independent of the rate or extent of the fluctuation of the symmetry axis. Thus the experimentally determined ratio $\langle \Delta\nu_{QL}/\Delta\nu_{QD} \rangle$ is a quantitative measure of the adequacy of a given model.

Table I lists the angles that the C-^{2}H bonds make with the symmetry axis (presumed to be the helix axis) as predicted by the different models. Although the dihedral angles for the models given in Table I are generally within 0.2 degrees of the values quoted in the literature (Chiu et al., 1990; Arseniev et al., 1985), certain discrepancies arise. For a regular helix in which the torsional angles for an L-D dipeptide were repeating, one would expect two splittings (one splitting for the left-handed amino acid C_α-^{2}H bond and the other for the right-handed amino acid label). However, variations of a degree or so in the angle between C_α-^{2}H bonds and the helix axis are expected even for the unrelaxed right- or left-handed

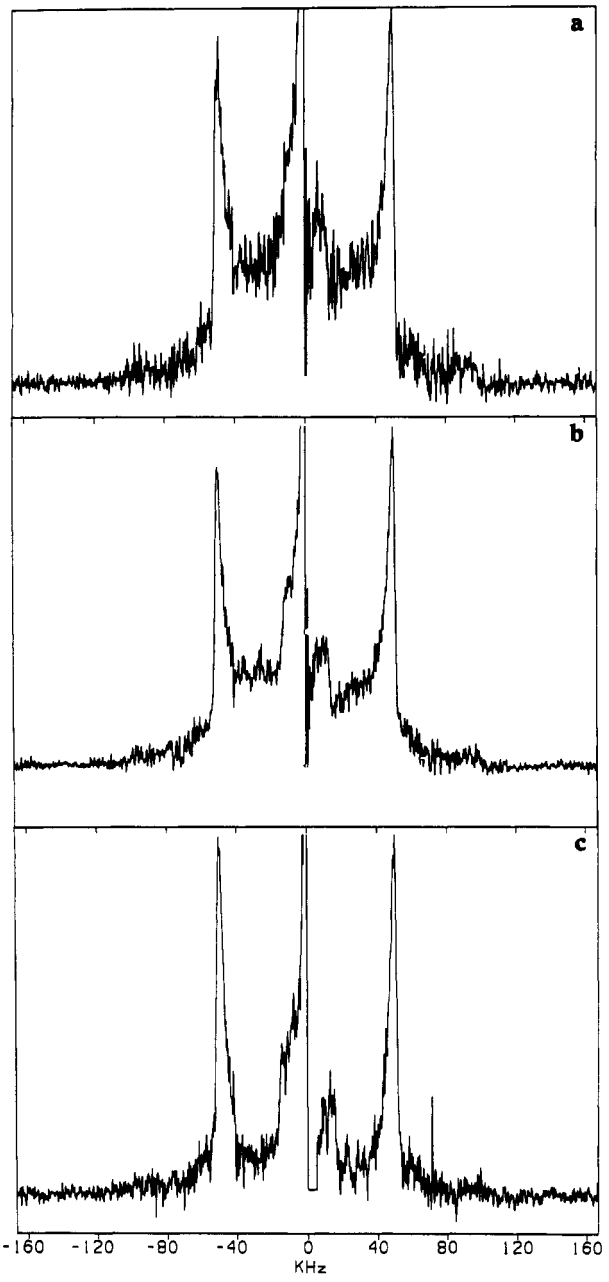

FIGURE 4: Quadrupolar echo spectra obtained from (^{2}H–C_α)Leu_{12} GA at 53.0 °C (a), 44.0 °C (b), and 20.6 °C (c). Each spectrum was acquired with 500 000 scans at 55.26 MHz.

$\beta_{LD}^{6.3}$ structures, since the angles between the C_α–^{2}H bond and the directly bonded carbon, nitrogen, or R-group atoms vary by a degree or so from one amino acid to the next. For example, for the case of the right-handed unrelaxed $\beta_{LD}^{6.3}$ helix, the predicted angles that the C_α–^{2}H bonds make with respect to the helix axis for the four leucine residues vary from 17.4° to 19.1°. Table I also lists the corresponding predicted quadrupolar splittings for all deuterons attached to the α carbons of the valine, alanine, leucine, or tryptophan residues or to the formyl-group carbon (the quadrupolar coupling constant is presumed to be e^2qQ/h = 168 kHz based on ^{2}H NMR spectra of the GA powders). In addition, the available experimentally determined quadrupolar splittings are included in Table I. Although the experimental quadrupolar splittings could be determined to an accuracy of a fraction of a kHz, a reasonable estimate for our experimental uncertainty is ±1 kHz, since there are two experimental data points for the quadrupolar splitting of (^{2}H–C_α)Ala_3 GA that differ by about 1 kHz, as can be seen from Table I. These data points were

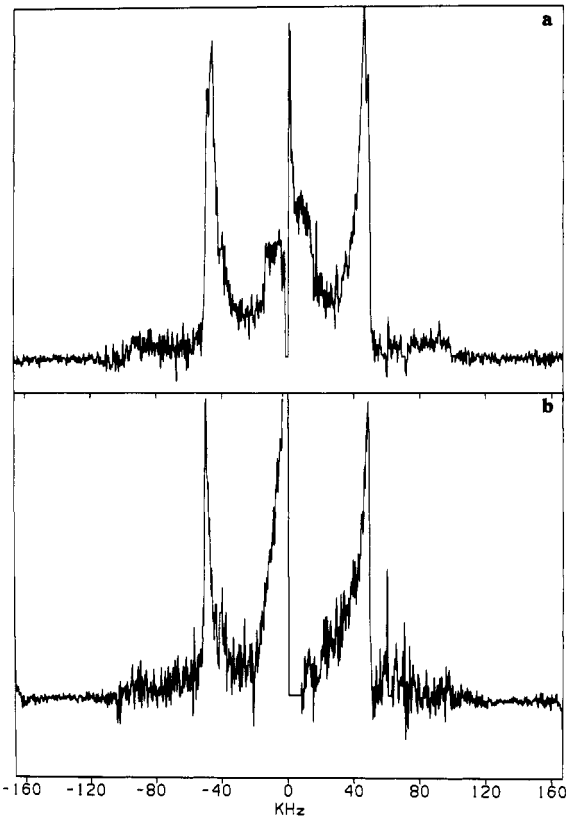

FIGURE 5: Quadrupolar echo spectra obtained from (^{2}H–C_α)Ala_3, (H^2–C_α)Ala_5 GA at 44 °C (a) and from (^{2}H–C_α)Ala_3 GA at 44 °C (b). The interpulse spacing τ was 35 μs in the first case and 25 μs in the second, while the doubly labeled sample was acquired through 600 000 scans and the singly labeled sample from 400 000 scans at 55.26 MHz.

obtained from a doubly labeled sample, (^{2}H–C_α)Ala_3, (^{2}H–C_α)Ala_5 GA, and a singly labeled species, (^{2}H–C_α)Ala_3 GA. This is shown in Figure 5, which displays quadrupolar echo spectra at 44 °C obtained from the doubly labeled (^{2}H–C_α)Ala_3, (^{2}H–C_α)Ala_5 GA (Figure 5a) and from (^{2}H–C_α)Ala_3 GA (Figure 5b). As is evident from the spectra, the outer splitting in Figure 5a agrees with the splitting of Figure 5b, to within 1 kHz. However, the average of the two measurements for Ala_3 (98.2 kHz) is significantly smaller than the observed splitting of 102.95 kHz reported by Hing et al. (1990a) for multilayers of (^{2}H–C_α)Ala_3 GA in DMPC at 44 °C. The work of Hing et al. differs from ours primarily in that their samples were oriented between glass plates and free of buffer. Figure 6 displays quadrupolar echo spectra at 44 °C of the GA molecules in which the right-handed amino acids have been labeled: (^{2}H–C_α)Leu_{14} GA (a), (^{2}H–C_α)Leu_{12} GA (b), (^{2}H–C_α)Leu_{10} GA (c), and (^{2}H–C_α)Leu_4 GA (d).

A number of conclusions can be drawn from the spectra in Figures 5 and 6. First, the typical powder-pattern profiles of the spectra indicate that for all of the GA labels gramicidin A is in the fast axially symmetric motional regime. Second, for all of the singly labeled species, the single sharp 90° doublet in each spectrum indicates that one major conformational state exists for each of the GA labels, with the possible exception of (^{2}H–C_α)Leu_{10} GA (Figure 6c) in which there may be a broad minor component whose splitting is roughly 117 kHz. This minor component was also observed in that same sample at 53 °C.

As can be appreciated from the pair of doublets in Figure 5a, which are barely resolved, if a second component (of less intensity than the major componet) exists, then it may not be resolvable if its splitting lies within roughtly ±5 kHz of the

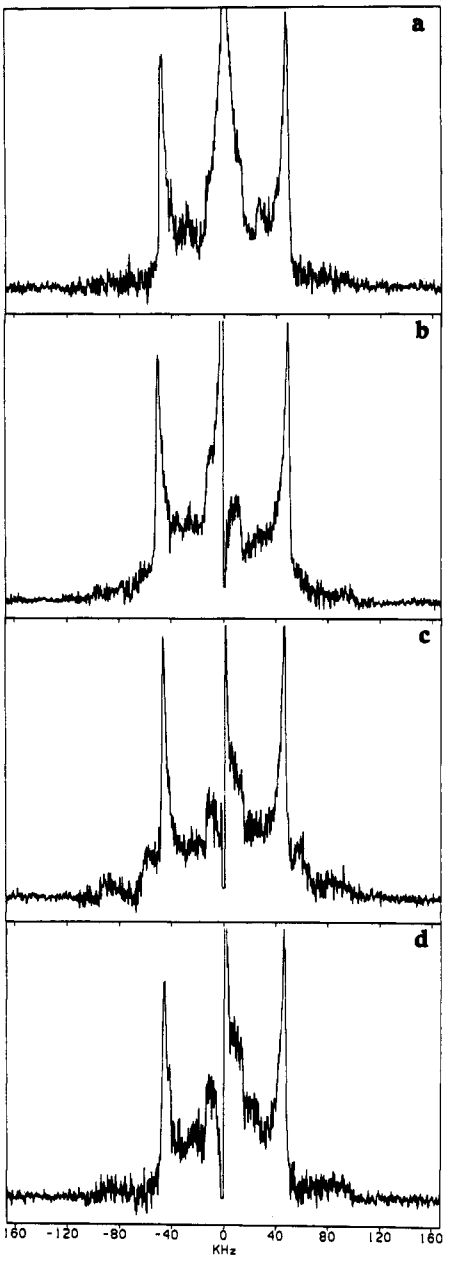

FIGURE 6: Quadrupolar echo spectra obtained from (^{2}H–C_α)Leu$_{14}$ GA (a), (^{2}H–C_α)Leu$_{12}$ GA (b), (^{2}H–C_α)Leu$_{10}$ GA (c), and (^{2}H–C_α)Leu$_4$ GA (d). These spectra were acquired through 650 000, 500 000, 800 000, and 600 000 scans, respectively, while τ was 35 μs in each case, taken at 55.26 MHz.

major component. In addition, if a minor component existed whose intensity was considerably less than that of the major component, it would likely be totally obscured by the major component. A difference of 5 kHz out of 110 kHz translates into an angular conformational change of roughtly ±3°. In order to estimate the possible distribution of angular conformations more accurately for the various GA labels, it would be better to prepare oriented multilayers and to employ proton decoupling. This has in fact already been accomplished with (^{2}H–C_α)Ala$_3$ GA (Hing et al., 1990a,b) in which the authors reported a line width at half maximum of less than 1 kHz at 44 °C; additionally, proton decoupling reduced the line width by a factor of 2 in the L_α phase. Apparently the ^{2}H–^{1}H dipolar interactions are a strong source of T_2 relaxation, although the advantages conferred to an unoriented system from proton decoupling may not be as great.

Assuming that the observed splittings represent a single average GA backbone conformer and that the molecules are

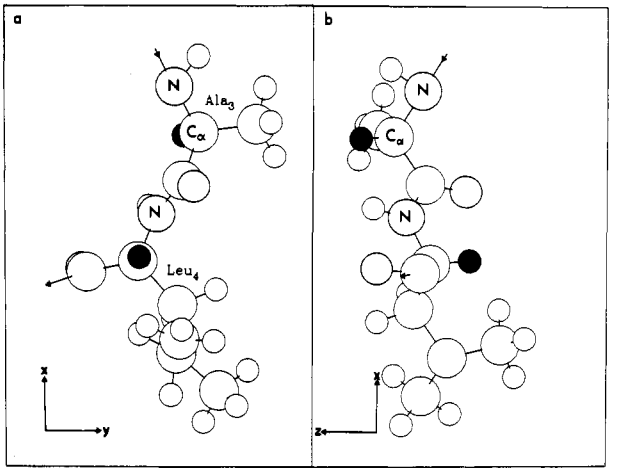

FIGURE 7: A ball-and-stick model representation of the Ala$_3$-Leu$_4$ dipeptide in GA using the coordinates from the relaxed right-handed $\beta^{6.3}_{LD}$ helix. The perspective in panel a is such that the helix axis is pointing directly into the page, while in panel b the helix axis is horizontal on the page. Note that the deuterons attached to the α carbon atoms have been shaded in. For clarity the atoms have been drawn such that their radii are 0.30 times their respective accepted van der Waals distances.

undergoing rapid axially symmetric reorientation, then the average ^{2}H–C_α bond orientation may be obtained once the extent of motional narrowing has been determined. One can see from eq 2 that there are two possible bond orientations for splittings less than 63 kHz; however, the splittings reported in this paper were all larger than this value. Thus, there is only one possible orientation of the ^{2}H–C_α bond (keeping in mind that $180 - \theta$ is the same as θ).

The ratio $\langle \Delta\nu_{QL}/\Delta\nu_{QD} \rangle$ is independent of narrowing effects caused by fluctuations of the symmetry axis, and as such this ratio is a good number to use as a test for the handedness of the helix. Figure 7 displays two perspectives of the Ala$_3$–Leu$_4$ dipeptide for the relaxed $\beta^{6.3}_{LD}$ helical model and clearly shows that the C_α–^{2}H bonds are roughly antiparallel to each other, while the magnitude of the acute angles, formed between the C_α–^{2}H bonds and the helix axis, are nearly equal. As can be seen from Table I, the unrelaxed left-handed $\beta^{6.3}_{LD}$ helical model predicts an average ratio of $\langle \Delta\nu_{QL}/\Delta\nu_{QD} \rangle = 0.90$, while for the relaxed left-handed Urry $\beta^{6.3}_{LD}$ helical model, seen on an MDS after 80 ps, a ratio of 0.91 is predicted (Chiu et al., 1990). For each model, we calculated this ratio by averaging over the eight possible combinations of $\Delta\nu_{QL}/\Delta\nu_{QD}$ from the residues that we have labeled (the two L-alanine residues, Ala$_3$ and Ala$_5$, and the four D-leucine residues, Leu$_4$, Leu$_{10}$, Leu$_{12}$, and Leu$_{14}$); the uncertainties quoted in Table I are the standard deviations from the mean. Note from Table I that the right-handed helices (the relaxed and unrelaxed $\beta^{6.3}_{LD}$ models and Arsenive's model) all predict a ratio of between 0.97 and 1.10 for $\langle \Delta\nu_{QL}/\Delta\nu_{QD} \rangle$. By comparison, our experimentally determined estimate of $\langle \Delta\nu_{QL}/\Delta\nu_{QD} \rangle$ is 1.01 ± 0.04. Evidently the data is consistent with a right-handed helix, in accordance with recent ^{15}N NMR results (Nicholson et al., 1989). The values for $\langle \Delta\nu_{QL}/\Delta\nu_{QD} \rangle$ predicted by either of the left-handed models (0.904 and 0.907) are not within one standard deviation of the experimentally determined value.

Table I also gives the predicted angle between the C–^{2}H bond for the deuteron attached to the formyl carbon and the symmetry axis. The corresponding splitting at this site turns out to be a discriminating test of the various models of the channel conformation of GA. Again, the results weigh in favor of a right-handed helix; Hing et al. (1990b) report that the splitting is 13.4 kHz, while we obtain theoretical values of 12.8,

Table I: Predicted Angles between the C–^{2}H Director and the Symmetry Axis, the Corresponding Quadrupolar Splittings, and the Experimentally Determined Splittings at 44 and 53 °C for GA Analogues[a]

label	left-handed $\beta_{LD}^{6.3}$		left-handed $\beta_{LD}^{6.3}$ run on MDS for 80 ps		right-handed $\beta_{LD}^{6.3}$		right-handed $\beta_{LD}^{6.3}$ run on MDS for 80 ps		right-handed Arseniev model		exptl $\Delta\nu_Q$ (kHz)	
	θ[b]	$\Delta\nu_Q$ (kHz)	θ	$\Delta\nu_Q$ (kHz)	θ	$\Delta\nu_Q$ (kHz)	θ	$\Delta\nu_Q$ (kHz)	θ[c]	$\Delta\nu_Q$ (kHz)	44 ± 1 °C	53 ± 1 °C
formyl ^{2}H–C	104.1	51.4	96.9	59.9	50.7	12.8	67.7	35.6	70.8, 107.0	42.3, 46.6	NA[d]	13.4[e]
^{2}H–C$_\alpha$ Val$_1$	18.4	106.4	18.6	106.0	166.7	115.8	165.2	113.1	159.8, 18.4	101.8, 106.6	NA	NA
^{2}H–C$_\alpha$ Ala$_3$	18.6	106.0	18.8	105.6	168.5	117.7	166.4	114.9	162.1, 15.8	107.5, 111.2	97.7,[f] 98.7[g]	95.1,[f] 96.3[g]
^{2}H–C$_\alpha$ Leu$_4$	168.0	117.1	167.4	116.3	17.4	108.5	10.7	118.7	15.4, 160.7	112.0, 104.6	91.8	91.3
^{2}H–C$_\alpha$ Ala$_5$	19.0	105.5	19.9	105.4	168.5	117.8	166.4	114.9	170.7, 12.9	120.3, 115.8	92.8[f]	90.9[f]
^{2}H–C$_\alpha$ Val$_6$	167.8	117.0	167.5	116.5	19.5	104.2	11.1	118.3	19.4, 161.5	104.4, 106.3	NA	NA
^{2}H–C$_\alpha$ Val$_7$	18.8	105.7	18.7	106.0	167.4	116.4	166.4	114.8	165.7, 14.9	113.7, 112.8	NA	NA
^{2}H–C$_\alpha$ Val$_8$	167.8	117.0	167.5	116.4	18.8	105.7	11.2	118.2	19.5, 162.1	104.4, 107.5	NA	NA
^{2}H–C$_\alpha$ Trp$_9$	17.4	108.2	17.9	107.1	168.6	118.0	166.1	114.4	165.2, 15.6	113.0, 111.7	NA	NA
^{2}H–C$_\alpha$ Leu$_{10}$	168.0	117.1	167.3	116.2	19.4	104.7	10.8	118.7	20.1, 156.6	103.1, 95.7	92.8	91.8
^{2}H–C$_\alpha$ Trp$_{11}$	17.9	107.2	18.0	107.4	166.8	115.5	166.0	114.2	168.2, 16.0	117.4, 110.9	NA	NA
^{2}H–C$_\alpha$ Leu$_{12}$	167.6	116.6	167.4	116.2	17.7	107.8	10.8	118.7	15.0, 165.2	112.6, 113.0	99.2	98.7
^{2}H–C$_\alpha$ Trp$_{13}$	18.5	106.6	18.0	107.4	169.0	118.4	166.0	114.2	172.0, 7.4	121.6, 122.1	NA	NA
^{2}H–C$_\alpha$ Leu$_{14}$	167.8	116.9	167.5	116.5	17.1	109.0	10.9	118.6	18.7, 164.2	106.0, 111.3	95.3	94.8
^{2}H–C$_\alpha$ Trp$_{15}$	18.0	107.3	16.9	107.6	169.2	118.7	166.0	114.2	157.2, 24.8	97.0, 93.4	NA	NA
$\langle\Delta\nu_{QL}/\Delta\nu_{QD}\rangle$	0.904 ± 0.003		0.907 ± 0.001		1.096 ± 0.017		0.968 ± 0.041		1.062 ± 0.053		1.01 ± 0.041[h]	

[a] The uncertainty in the quadrupolar splittings is discussed in the text. [b] θ refers to the angle between the ^{2}H–C$_\alpha$ bond and the helix axis. [c] As is evident from Figure 1, there is an apparent kink in the Arseniev dimer model. Hence generally a different value of θ is obtained from each monomer, and a distribution of angles between the two is expected. [d] NA means not available. [e] This experimental data point came from Hing (1990). [f] This splitting was obtained from a doubly labeled sample (^{2}H–C$_\alpha$)Ala$_3$, (^{2}H–C$_\alpha$)Ala$_5$ GA. [g] This splitting was obtained from a singly labeled species (^{2}H–C$_\alpha$)Ala$_3$ GA. [h] This estimate was obtained from spectra at 44 °C.

Table II: Predicted Motionally Narrowed Splittings for GA Analogues

label	left-handed $\beta_{LD}^{6.3}$ $\Delta\nu_Q$ (kHz)	left-handed $\beta_{LD}^{6.3}$ run on MDS for 80 ps $\Delta\nu_Q$ (kHz)	right-handed $\beta_{LD}^{6.3}$ $\Delta\nu_Q$ (kHz)	right-handed $\beta_{LD}^{6.3}$ run on MDS for 80 ps $\Delta\nu_Q$ (kHz)	right-handed Arseniev model ν_Q (kHz)	exptl $\Delta\nu_Q$ (kHz)
^{2}H–C$_\alpha$ Ala$_3$	88.8	88.8	100.6	93.0	94.7	98.2
^{2}H–C$_\alpha$ Leu$_4$	98.1	97.8	92.8	96.0	93.8	91.8
^{2}H–C$_\alpha$ Ala$_5$	88.3	88.7	100.7	93.0	102.2	92.8
^{2}H–C$_\alpha$ Leu$_{10}$	98.1	97.7	89.5	96.0	86.1	92.8
^{2}H–C$_\alpha$ Leu$_{12}$	97.6	97.7	92.2	96.0	97.7	99.2
^{2}H–C$_\alpha$ Leu$_{14}$	97.9	98.0	93.2	95.9	94.1	95.3
$\sum_i(\Delta\nu_{Qi}^{predict} - \Delta\nu_{Qi}^{exp})^2$	185.7 kHz^2	174.7 kHz^2	133.5 kHz^2	65.6 kHz^2	153.2 kHz^2	

35.6, 42.3, and 46.6 kHz for the right-handed $\beta_{LD}^{6.3}$ helix without and with MDS and for each of the two monomers of the Arseniev model, respectively. The left-handed helical models predict splittings of 51.4 and 59.9 kHz. While the prediction for the splitting based on the right-handed $\beta_{LD}^{6.3}$ helix is less than the experimentally determined value, a change of only a couple of degrees in the orientation of the formyl C–^{2}H bond from the right-handed $\beta_{LD}^{6.3}$ conformation would then be consistent with experiment. The other models (particularly the left-handed models) would require a fairly substantial conformational change in the formyl C–^{2}H bond direction or substantial motional narrowing (or both) in order to be consistent with the data.

Although the ratio $\langle\Delta\nu_{QL}/\Delta\nu_{QD}\rangle$ is useful for determining the handedness of the helix, it is preferrable to invoke the entire set of predicted splittings, for which there is a corresponding set of experimental splittings, in order to discriminate among the various conformational models. If we assume that the only motions of the GA dimer, on the ^{2}H NMR time scale, are fast diffusion about the helix or symmetry axis and reorientations of the helix (symmetry) axis with respect to the external magnetic field, then we are justified in multiplying the set of predicted splittings by a single motional-narrowing factor. This was done for all five models although, in the case of the Arseniev model, the predicted splitting was an average from both monomers. (For the Arseniev model each of the monomers ends up being slightly tilted from the average helix axis in order for the intermonomer hydrogen bonds to be energetically optimized. This scenario of slightly tilted monomers may be unrealistic in a bilayer where the orienting potential due to the lipid matrix would tend to align the monomers.) Each set of predicted splittings for a given model was multiplied by the "motional-narrowing" scaling factor that produced the best fit with the data. The results of these fits are given in Table II, where predicted splittings are given for each model. The last row in Table II gives the sum of the squares of the differences between the predicted splittings and the experimentally determined splittings for each model. These numbers indicate that although the right-handed models fare better than either of the left-handed models, the best fit with the data arises from the relaxed right-handed $\beta_{LD}^{6.3}$ helix. In the case of the relaxed right-handed $\beta_{LD}^{6.3}$ helix model, no predicted splitting was off by more than 5.2 kHz from the experimentally determined value, which for splittings on the order of 100 kHz translates into a change in orientation of roughly 5°. Obviously it is difficult at present to distinguish further among the right-handed models without spectra for deuterons attached to the α carbons of the other residues in GA.

The spectra indicate that the two monomers are equivalent, i.e., the labels on both monomers give the same quadrupolar splitting to within the line width (of the order of 1 kHz). If we assume that the dimer is rigid and undergoes rapid axially symmetric reorientation, then it should be possible to use the observed splittings to determine the axis of motional averaging

if we know the molecular structure. In addition, we need to allow for a wobble of the axis of motion relative to the bilayer normal. After each set of predicted splittings is multiplied by the optimal motional-narrowing factor to account for this wobble, the most appropriate motional axis is determined to be that which gives a minimum for the sum of the squares of the differences between the predicted splittings and the experimental splittings. We have tested the predictions of the above models and find that in all cases the best agreement with our experimental splittings is obtained with the motional axis lying very close to the helix axis. In the case of the relaxed right-handed helix, for example, the motional axis is within 0.3° of the helix axis.

If the peptide backbone segments closest to the membrane surface possessed greater motional freedom than those near the center, then it is anticipated that this local flexibility would be manifested as an additional motional narrowing of the components from the outer turn of the helix (Leu_{10}, Leu_{12}, or Leu_{14}). However the correspondence between the splittings predicted by the relaxed right-handed $\beta^{6.3}_{LD}$ helix and the observed splittings, for labels from both the inner and outer turn of Ga, did not reflect a peptide-backbone flexibility gradient. In the presence of helical librations of the kind discussed by Smith et al. (1989), significant fluctuations in the orientations of C=O groups (or N-H groups) would be expected, while the positions of the α carbons could remain relatively fixed. To test this hypothesis, four right-handed helically librated conformers were generated with MACROMODEL (Columbia University, NY) and oriented by eye by using the torsional angles given by Venkatachalam and Urry (1985). The angles formed by the C_α–H bonds and the helix axis were found to be within 5° of the average values, whereas the C=O groups deviated by as much as 20° from their average angles. It is therefore possible that the local C=O librations are more extensive close to the membrane surface, while deviations in the orientation of adjacent C_α–H bonds would be considerably more restricted.

Conclusions

Solid-state NMR is an effective means of obtaining structural and dynamical information on the channel conformation of GA in a biological membrane. When applied to GA labels in which certain α-carbon protons have been replaced with deuterium, ^{2}H NMR has the additional advantage over most other solid-state NMR techniques that the transformation from the principal axis system to the molecular coordinate system is trivial, since η is effectively zero and V_{zz} lies along the C–^{2}H bond. For this reason, quadrupolar splittings obtained from unoriented multilamellar dispersions yield direct orientational constraints on the C–^{2}H bond under study. The quadrupolar echo spectra of all the GA labels studied thus far were found to be in the fast motional regime on the ^{2}H NMR time scale.

In all of the spectra obtained, evidence was found for a single well-defined conformation. In spectra of powder samples for which there is no proton decoupling, the line width makes it difficult to estimate orientational dispersion in the peptide backbone. Therefore less populated conformational substates in which the ^{2}H–C_α bond orientation was different by only a few degrees from the observed average conformation may exist.

From measurements of the average ratio of the quadrupolar splitting of a left-handed amino acid label to that of a right-handed label $\langle \Delta\nu_{QL}/\Delta\nu_{QD} \rangle$, we conclude that the helix sense of GA is right-handed, in agreement with the conclusions from ^{15}N NMR by Nicholson and Cross (1989). The left-handed $\beta^{6.3}_{LD}$ models yielded an average ratio for $\langle \Delta\nu_{QL}/\Delta\nu_{QD} \rangle$ that was significantly less than the experimentally determined ratio, whereas the right-handed relaxed $\beta^{6.3}_{LD}$ and Arseniev models yielded average ratios that were within the uncertainty limits of the experimental value.

Assuming that the only motions are fast axially symmetrric diffusion of the GA molecule as a whole about its helical (or average helical) axis and reorientations of the axis of motional symmetry with respect to the local bilayer normal, then the theoretical splittings for a given model may all be scaled by a constant motional narrowing factor that gives the best fit to experimental splittings. The relaxed right-handed $\beta^{6.3}_{LD}$ helix, run on MDS for 80 ps (Chiu et al., 1990), was found to give the best fit to the experimental results. The axis of motional averaging was further determined to be roughly colinear with the presumed helix axis. Also, on the basis of an absence of additional narrowing for labels from the outer turn of the backbone, no additional flexibility was observed in the outer turn. This is not in contradiction with the findings of Smith et al. (1989) if the fluctuations they observed in the carbonyl groups are attributed to local carbonyl librations.

In a recent paper, Brenneman and Cross (1990) suggested that by using both ^{15}N–^{1}H, ^{15}N–$^{13}C_1$ dipolar and chemical shift information and ^{2}H NMR of the protons attached to the α carbons of all backbone residues, the number of admissable backbone conformations of the gramicidin channel would be sufficiently manageable for a computer to select the most likely structure via an energetic analysis approach. Solid-state NMR is in general a model-dependent technique and as such the collaborative efforts of experimental work on more than one magnetic nucleus along with such theoretical work will likely prove to be the most rewarding.

Acknowledgments

Our thanks to Dr. Rick Yada and to Massimo Marcone of the Department of Food Science, University of Guelph, for assistance in the circular dichroism experiments and to Dr. M. Morrow for his part in writing the contraction program and for his critical reading of the manuscript. Thanks to Lawrence MacIntosh and Mike Strain for their help with the 2D COSY experiments Special thanks to Prof. Jakobsson and to M. Brenneman at the University of Chicago for providing the computer generated models used in this paper. Thanks to Prof. R. Norberg and Dr. A. Hing for providing us with a copy of A. Hing's Ph.D. thesis. Also we thank Cynthia Fields, Applied Biosystems, for providing details on the solid-phase synthesis and chromatography prior to publication.

Registry No. DMPC, 18194-24-6; gramicidin A, 11029-61-1.

References

Åqvist, J., & Warshel, A. (1989) *Biophys. J. 56*, 171–182.

Arseniev, A., Barsukov, I., Bystrov, V., Lomize, A., & Ovchinnikov, Y. (1985) *FEBS Lett. 186*, 168–174.

Bidlingmeyer, B. A., Cohen, S. A., & Tarvin, T. L. (1984) *J. Chromatogr. 336*, 93–104.

Brenneman, M., & Cross, T. (1990) *J. Chem. Phys. 92*, 1483–1494.

Chapman, D., Cornell, B, Eliaxz, W., & Perry, A. (1977), *J. Mol. Biol. 113*, 517–538.

Chiu, S., Nicholson, L., Brenneman, M., Subramanium, S., Teng, Q., North, C., McCammon, J., Cross, T., & Jakobsson, E. (1990) *Biophys. J. 57*, 101a.

Cornell, B. A., & Separovic, F. (1988) *Eur. Biophys. J. 16*, 299–306.

Cornell, B. A., Separovic, F., Baldassi, A., & Smith, R. (1988) *Biophys. J. 53*, 67–76.

Cornell, B. A., Separovic, F., Thomas, D., Atkins, A., &

Smith, R. (1989) *Biochim. Biophys. Acta 985*, 229–232.
Datema, K., Pauls, K., & Bloom, M. (1986) *Biochemistry 25*, 3796–3803.
Davis, J. (1983) *Biochim. Biophys. Acta 737*, 117–171.
Davis, J. (1988) *Biochemistry 27*, 428–436.
Davis, J., Jeffrey, K., Bloom, M., Valic, M., & Higgs, T. (1976) *Chem. Phys. Lett. 42*, 390–394.
Deisenhofer, J., Epp, O., Miki, K., Huber, R., & Michel, H. (1985) *Nature 318*, 618–624.
Ernst, R. R., Bodenhausen, G., & Wokaun, A. (1987) *Principles of Nuclear Magnetic Resonance in One and Two Dimensions*, Oxford University Press, Oxford.
Fields, C. G., Fields, G. G., Noble, R. L., & Cross, T. A. (1989) *Int. J. Pept. Protein Res. 33*, 298–303.
Gennis, R. (1989) *Biomembranes* (Cantor, C. R., Ed.) pp 101–105, Springer-Verlag, New York.
Greenstein, J. P., & Winitz, M. (1961) *Chemistry of the Amino Acids*, Vols 1–3, John Wiley and Sons, New York.
Heinemann, S., & Sigworth, F. (1989) *Biochim. Biophys. Acta 987*, 8–14.
Hing, A., Adams, S., Silbert, D., & Norberg, R. (1990a) *Biochemistry 29*, 4144–4156.
Hing, A., Adams, S., Silbert, D., & Norberg, R. (1990b) *Biochemistry 29*, 4156–4166.
Hinton, J., Fernandez, J., Shungu, D., Whaley, W., Koeppe, R., & Millett, F. (1988) *Biophys. J. 54*, 527–533.
Hinton, J., Fernandez, J., Shungu, D., & Millett, F. (1989) *Biophys. J. 55*, 327–330.
Killian, J., & Urry, D. (1988) *Biochemistry 27*, 7295–7301.
Killian, J., Prasad, K., Urry, D., & de Kruijff, B. (1989) *Biochim. Biophys. Acta 978*, 341–345.
Koeppe, R., Mazet, J., & Andersen, O. (1990) *Biochemistry 29*, 512–520.
LoGrasso, P., Moll, F., & Cross, T. (1988) *Biophys. J. 54*, 259–267.
Macdonald, P., & Seelig, J. (1988) *Biochemsitry 27*, 2357–2364.
Masotti, L., Spisni, A., & Urry, D. (1980) *Cell Biophys. 2*, 241–251.
Moll, F., & Cross, T. (1990) *Biophys. J. 57*, 351–362.
Morrow, M., & Davis, J. (1988) *Biochemistry 27*, 2024–2032.
Nicholson, L., & Cross, T. (1989) *Biochemistry 28*, 9379–9385.
Nicholson, L., LoGrasso, P., & Cross, T. (1989) *J. Am. Chem. Soc. 111*, 400–401.
Nielsen, K. L. (1964) *Methods in Numercial Analysis*, MacMillan, New York.
Opella, S., & Stewart, P. (1989) *Methods Enzymol. 176*, 242–275.
Oppenheim, A. V., & Schafer, R. W. (1975) *Digital Signal Processing*, Prentice-Hall, Englewood Cliffs, NJ.
Roux, B., & Karplus, M. (1988) *Biophys. J. 53*, 297–309.
Sarges, R., & Witkop, B. (1965) *Biochemistry 4*, 2491–2494.
Sawyer, D., Koeppe, R., & Andersen, O. (1990) *Biophys. J. 57*, 515–523.
Smith, R., Thomas, D., Separovic, F., Atkins, A., & Cornell, B. (1989) *Biophys. J. 56*, 307–314.
Stankovic, C., Delfino, J., & Schreiber, S. (1990) *Anal. Biochem. 184*, 100–103.
Stewart, J. M., & Young, J. D. (1984) *Solid Phase Peptide Synthesis*, Pierce Chemical Co., Rockford, IL.
Strässle, M., Stark, G., Wilhelm, M., Daumas, P., Heitz, F., & Lazaro, R. (1989) *Biochim. Biophys. Acta 980*, 305–314.
Tanaka, H., & Freed, J. (1985) *J. Phys. Chem. 89*, 350–360.
Traficante, N. (1987) *J. Magn. Reson. 71*, 237–245.
Urry, D., Goodall, M., Glickson, J., & Mayers, D. (1971) *Proc. Natl. Acad. Sci. U.S.A. 68*, 1907–1911.
Urry, D., Walker, J., & Trapane, T. (1982) *J. Membr. Biol. 69*, 225–231.
Van Mau, N., Trudelle, Y., Daumas, P., & Heitz, F. (1988) *Biophys. J. 54*, 563–567.
Vankatachalam, C., & Urry, D. (1983) *J. Comput. Chem. 4*, 461–469.
Venkatachalam, C., & Urry, D. (1984) *J. Comput. Chem. 5*, 64–71.
Wallace, B. (1983) *Biopolymers 22*, 397–402.
Wallace, B. A., & Ravikumar, K. (1988) *Science 241*, 182–187.
Wang, S., Martin, E., Cimino, J., Omann, G., & Glazer, M. (1988) *Biochemistry 27*, 2033–2039.
Watnick, P., Chan, S., & Dea, P. (1990) *Biochemistry 29*, 6215–6221.